Hindawi
Journal of Nanotechnology
Volume 2017, Article ID 9289273, 8 pages
https://doi.org/10.1155/2017/9289273

Research Article

Structure and Electrochemical Properties of a Mechanochemically Processed Silicon and Oxide-Based Nanoscale Composite as an Active Material for Lithium-Ion Batteries

Norihiro Shimoi and Kazuyuki Tohji

Graduate School of Environmental Studies, Tohoku University, 6-6-20 Aoba, Aramaki, Aoba-ku, Sendai 980-8579, Japan

Correspondence should be addressed to Norihiro Shimoi; norihiro.shimoi.c8@tohoku.ac.jp

Received 24 December 2016; Accepted 23 February 2017; Published 9 March 2017

Academic Editor: Cheng Yan

Copyright © 2017 Norihiro Shimoi and Kazuyuki Tohji. This is an open access article distributed under the Creative Commons Attribution License, which permits unrestricted use, distribution, and reproduction in any medium, provided the original work is properly cited.

Si is essential as an active material in Li-ion batteries because it provides both high charge and optimal cycling characteristics. A composite of Si particles, Cu particles, and pure H_2O was realized to serve as an anode active material and optimize the charge–discharge characteristics of Li-ion batteries. The composite was produced by grinding using a planetary ball mill machine, which allowed for homogenous dispersion of nanoscale Cu_3Si as Si–Cu alloy grains and nanoscale Si grains in each poly-Si particle produced. Furthermore, some Si particles were oxidized by H_2O, and oxidized Si was distributed throughout the composite, mainly as silicon monoxide. As a result, each Si particle included silicon monoxide and conductive Cu_3Si materials, allowing for effective optimization of the recharging and charge-discharge characteristics. Thus, a new and simple process was realized for synthesizing a Si active material composited with silicon oxides, including silicon monoxide. This Si-rich conductive material is suitable as an anode for Li-ion batteries with high charge and optimized cycling properties.

1. Introduction

Owing to its high theoretical Li storage potential of about 4000 mAh g^{-1} [1], Si is one of the most attractive anode materials for Li-ion batteries (LIBs). However, Si undergoes frequent drastic changes in volume during charge-discharge cycling, causing degradation of Si materials and drastically decreasing ionic and electronic conductivities, which has prevented Si anodes from being utilized in Li-ion secondary batteries [2]. To overcome this problem, various modifications, such as the use of nanostructured Si anodes, the synthesis of composites with other materials, and the use of carbon coatings, have been suggested [3–5]. The use of Si monoxide as an alternative anode material has been proposed [6–11], as Si monoxide exhibits little change in volume and high conductivity. However, the capacity of Si monoxide is only about 1200 mAh g^{-1}, which is lower than that of other potential materials [12, 13]. Numerous attempts have been made to find ways to compensate for this by combining Si monoxide with other materials [14–17].

This study considers a technique that maintains the high ionic and electronic conductivities of Si by preventing cracking during volume changes, with as little effect as possible on the capacity of the material. Namely, particles of an active material based on Si were formed into the core of a suitable conductive material and the Si crystal structure was controlled by compositing Si particles with other materials. To achieve this, we designed a composition including Si, Si oxide, and a conductive material, which could be employed as an anode electrode in LIBs. In this study, to synthesize a composite of Si and other materials, we used a grinding process to combine Si with H_2O as an oxidant and Cu as a conductive material. The grinding method was considered the most likely method to achieve a composite containing a homogeneous distribution of nanoscale Si and conductive materials. It was expected that a Si oxide with a

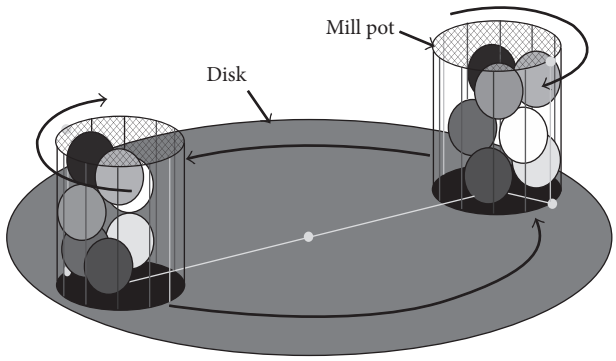

Figure 1: Schematic of the mechanics of a planetary ball mill.

low Si oxidation number would be formed by grinding with H_2O, resulting in the transfer of oxygen atoms the Si and Si particles. Moreover, a composite material containing Si oxide, Cu, and Si is expected to yield good performance with regard to charge-discharge characteristics.

In this study, we developed a grinding method in which Si particles (average diameter of 4 μm, purity of 99.999%; Kojundo Chemistry Laboratory Co., Ltd., Japan) and Cu particles (average diameter of 4 μm; Kojundo Chemistry Laboratory Co., Ltd., Japan) as a conductive material were ground with pure H_2O in the mill pots of a planetary ball mill (Fritsch Pulverisette-7) to produce a composite material. A mixture of approximately 2 g was put in a zirconia mill pot with a 45 cm^3 inner volume with 7 zirconia balls of 15 mm diameter and subjected to grinding using the planetary ball mill, as shown in Figure 1, at approximately 600 rpm in air. The mill pots rotated individually on a rotating disk. The crushing conditions were varied by changing the amounts of Cu, pure H_2O, and Si particles, as well as the grinding time. Table 1 shows the amounts of Si, H_2O, and Cu used in this study to prepare composites by grinding. The "X" values in Table 1 indicate the ratio of oxide atoms in the prepared composite relative to Si. The amount of Cu was constant based on the conditions for grinding Si and CuO [18]. Crushing and reconstruction of materials in the mill pot was expected to result in the formation of a composite containing Si, Cu, and oxidized species. Oxidation reactions that result in the transfer of an oxygen atom from H_2O to Si would produce a Si suboxide in the composite with Si and Cu. Further, residual Cu can serve as an electrically conductive material. Such composites synthesized from Si, H_2O, and Cu could then be employed as the active material in LIB anodes.

1.1. Characterization of Composite Material. Scanning electron microscopy (SEM; Hitachi High-Technologies Corporation, Japan) was used to examine the morphology of the composite particles. A composite-coated electrode was cut using a Ga focused ion beam (FIB; Hitachi High-Technologies Corporation, Japan) at an accelerating voltage of 5 kV. Scanning transmission electron microscopy (STEM; Hitachi High-Technologies Corporation, Japan) was carried out at an accelerating voltage of 200 kV to image cross sections of the electrode. The atomic distribution of Si, oxides, and Cu was measured using energy dispersive X-ray spectroscopy (EDX; Hitachi High-Technologies Corporation, Japan). The crystallization state of the ground composite was examined using X-ray diffraction (XRD; Rigaku Co. Japan). Electron energy-loss spectroscopy (EELS; Hitachi High-Technologies Corporation, Japan) at 200 kV was used to measure the distribution of oxides in the composite at a resolution of 0.5 eV. The EELS map was constructed from spectral images in the energy-loss region of 200–2200 eV, as detected using multiple charge-coupled devices. High-resolution Si2p X-ray photoelectron spectroscopy (XPS; Bruker) with a monochromatic AlKα X-ray source, an analysis range of 0.62 mm in diameter, and a detection angle of 45° was used to determine the oxidation number of Si in the composite particles. The composite particles were ground uniformly on a XPS sample holder, and measurements were obtained for the flattest section.

1.2. Anode Preparation and Electrochemical Testing. Anode electrodes for LIBs were prepared using the composites of Si, H_2O, and Cu as follows. Composite particles were mixed with a binder composed of polyamic acid (Ube-Kousan KK, Japan) and acetylene black (AB; Denkikagaku Kogyo KK, Japan) as a conductive material in a 1-methyl-2-pyrrolidone (NMP) solution. The weight ratio of composite particles : binder : AB was 70 : 20 : 10. To form electrodes, this slurry was cast onto a Cu foil and dried at 70°C for 30 min in air. The coated electrodes were cut to a size of 10 mm ϕ with a 78.5 mm^2 area. The electrode thickness was within the range of 40–50 μm. The electrodes were further sintered at 650°C under vacuum for 3 h and then pressed at 200 kgf cm^{-2}. The specific capacity was calculated according to the weight of Si in the composite particles.

Electrochemical testing of the composite electrodes was conducted using two-electrode test coin cells (2032-type, Housen, Japan) with caulked metal cups and a gasket to hold the electrode assembly and a separator. The coin cells were assembled in an Ar-filled glove box using a 1 M lithium hexafluorophosphate ($LiPF_6$) electrolyte in a mixed solution of ethylene carbonate (EC), diethylene carbonate (DEC), and dimethyl carbonate (DMC) (60 : 25 : 15, v/v). An Al foil coated with a $LiCoO_2$ film (320 μm thickness) with a capacity of 4.5 mAh cm^{-2} was employed as the cathode counter electrode, with a polyethylene/polypropylene/polyethylene multistacked film separator (40 μm thickness). The cathode electrode, separator, and anode electrode were not pressed before assembly in the test coin cell and were held in place by a leaf spring. The electrochemical performance of these two-electrode test coin cells was evaluated using a constant current charge-discharge cycling test in the voltage range of 1.6–4.2 V, with a current density of 0.1 mA cm^{-2} at room temperature.

2. Results and Discussion

2.1. Characterization of the Composite. In this study, we obtained composite particles by grinding Si, H_2O, and Cu (1.88 g Si, 0.12 g H_2O, and 0.28 g Cu; Table 1) in a planetary

Table 1: Amounts of Si, H_2O, and Cu used in the grinding process.

Si : O = 10 : X	0	0.33	0.5	0.75	1	1.3	1.5	3
Si (g)	2.0	1.95	1.94	1.91	1.88	1.84	1.82	1.68
H_2O (g)	0	0.05	0.06	0.09	0.12	0.16	0.18	0.32
Cu (g)	0.28	0.28	0.28	0.28	0.28	0.28	0.28	0.28

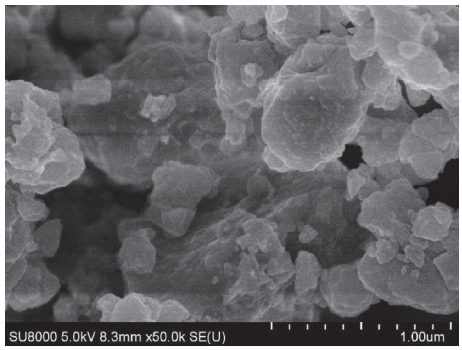

Figure 2: SEM image of microscale composite particles formed by grinding Si, H_2O, and Cu.

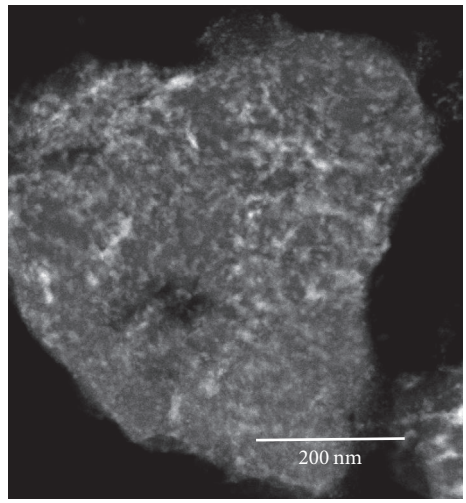

Figure 3: STEM cross-sectional dark field image of a composite-coated anode cut using a Ga FIB.

ball mill machine for a total of 3 h to obtain a homogeneous distribution of each component (Si, O, and Cu) in the composite. The molar ratio of Si : O in the composite was controlled at 10 : 1. The SEM images in Figure 2 reveal the composite particles obtained after grinding Si, H_2O, and Cu. The composite particles, which are similar in size to the bare Si particle, appear to have small particles attached along their circumferences. The composite particles were from 0.1 to 3.8 μm in size with an existence probability of 95%, and the medium diameter was 1.6 μm. Further, the average tapping density measured for the prepared sample was 2.19 g cm^{-3}, which is comparable to the tapping density of Si (approximately 2.3 g cm^{-3}).

An electrode coated with a mixture of composite particles, conductive materials, and a binder was cut using a Ga FIB to analyse electrode cross sections by STEM. The dark field image of the sliced anode electrode (Figure 3) shows dark grey areas corresponding to Si components and white areas corresponding to Cu or Cu components. Thus, it was revealed that the Si composites were homogeneously mixed with Cu materials. Punctate white regions were also observed in the composite materials, and we surmised that the composites were synthesized from a mixture of materials based on Si, H_2O, and Cu. EDX was used to measure the atomic distribution of Si, oxides, and Cu (Figure 4) in the composite. These results show that the material obtained following the grinding process contains both Si and Cu nanograins.

Figure 5 shows a high-resolution STEM image at 2000 K magnification of the area of the composite indicated by a white circle in the inset. The sample composition was observed as aggregates of nanoscale grains based on individual Si and Si–Cu composite materials. The bright grey areas, indicated by white arrows in Figure 5, are occupied by Si materials, whereas the dark grey areas, indicated by black arrows, contain Cu materials. The directions of these arrows indicate the orientation of each Si or Cu crystal lattice. Thus, high-resolution STEM imaging confirms that each grain has a random crystal orientation and that the composite mainly comprises poly-Si and Si–Cu composite nanograins.

The crystallization state of the ground composite was examined using XRD, as shown in Figure 6. Only Si and Cu particles were observed before the grinding process, whereas in the composite obtained after grinding, crystal patterns were observed that correspond to Si and Cu_3Si as a Si–Cu alloy [19]. Most oxygen atoms from H_2O were transferred to Si by the grinding process; on the other hand, Cu did not react with H_2O directly. These results confirm that the material obtained by grinding is a composite constructed of aggregated nanoscale grains of Si, Si oxidation materials, and Cu_3Si materials.

The distribution of oxides in the composite was measured using EELS. The EELS map obtained from STEM images is shown in Figure 7. Owing to oxidation reactions initiated by the grinding process, most oxygen atoms from H_2O were incorporated with Si into Si oxides. The EELS map in Figure 7, which is constructed from the spectral data at energy losses between 532 and 570 eV, implies that the distribution of oxide species, indicated by white dots, is not homogeneous in the composite. Thus, oxide species are concentrated near the surface of the composite particle, although some oxides also exist inside the particle.

The Si oxidation number of the composite particles was determined using high-resolution Si2p XPS spectroscopy.

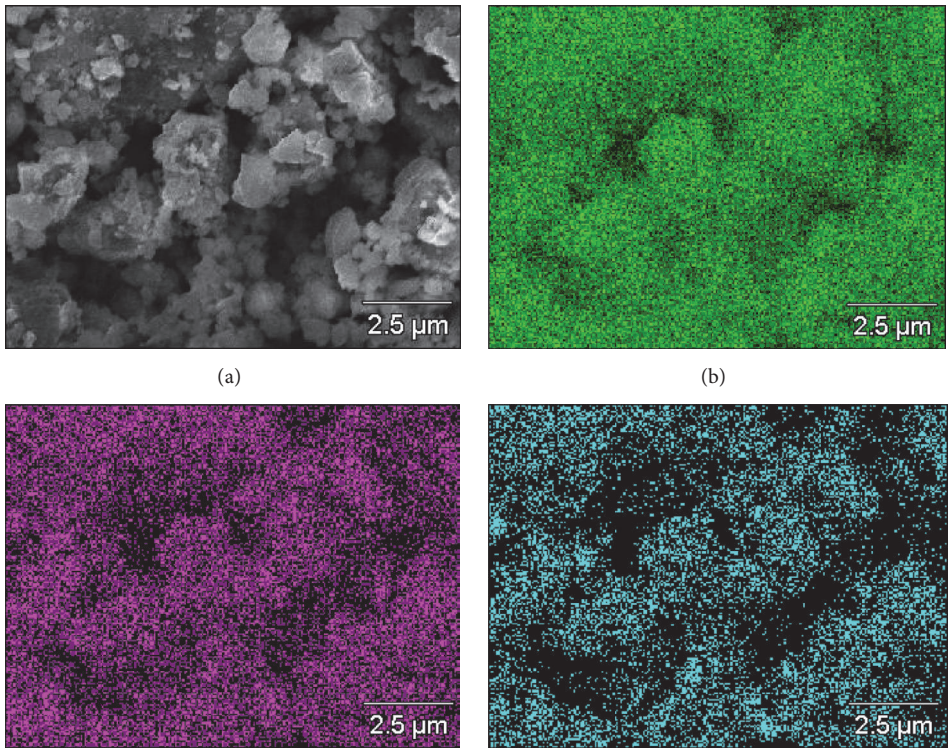

Figure 4: (a) STEM bright field image of the composite material and corresponding EDX distribution maps for (b) Si, (c) O, and (d) Cu.

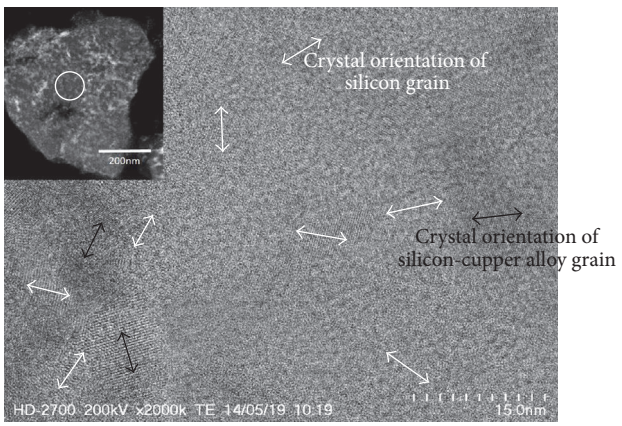

Figure 5: High-resolution STEM image of the composite (in the area indicated by a white circle in the inset) showing the presence of Si and Si–Cu alloy materials.

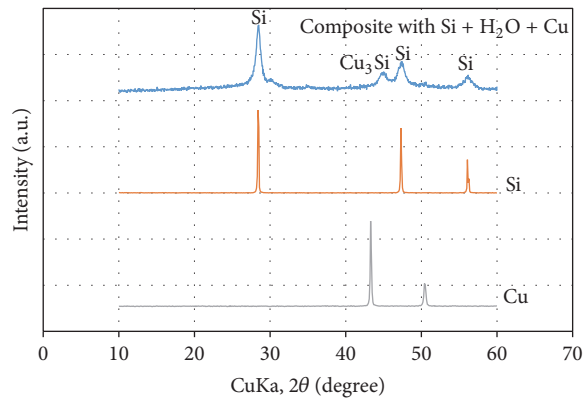

Figure 6: XRD patterns of the Si, H_2O, and Cu composite after the grinding process and Si and Cu particles before the grinding process.

The binding energies of the peaks in the XPS spectra were extrapolated by fitting with the Voigt profile [20–22]. The peak corresponding to carbon contaminants was employed as a reference for the binding energy. The XPS results shown in Figure 8 indicate that the composite contains a variety of Si ions with different oxidation numbers. The Si2*p* peaks located at higher binding energies (~100–104 eV) mainly correspond to Si-suboxide species: Si^{4+}, Si^{3+}, Si^{2+}, and Si^{1+}. The content ratios of the different Si ions in the composite particles were calculated by deconvolution of the peak, which was calibrated against the C1*s* signal. In addition, each Si oxidation number was evaluated by calculating the chemical shift distribution based on the results shown in Figure 8. Si in the composite particles is mainly Si^0 (Si); however, the distribution of the binding energies indicates that the composite also contains some oxidized Si species: Si^{4+}, Si^{3+}, Si^{2+}, and Si^{1+}. This finding confirms the existence of a semisilicate, similar to Si monoxide, near the surface

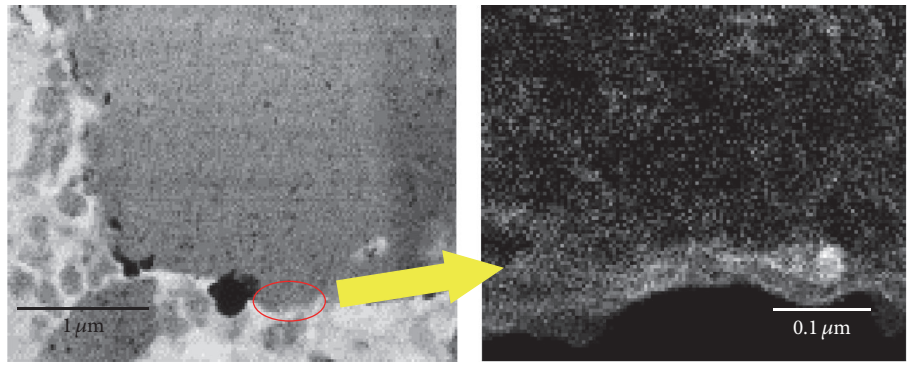

FIGURE 7: (a) STEM bright field image of the composite and (b) EELS map of the distribution of oxides in the composite for the area in the red circle in (a).

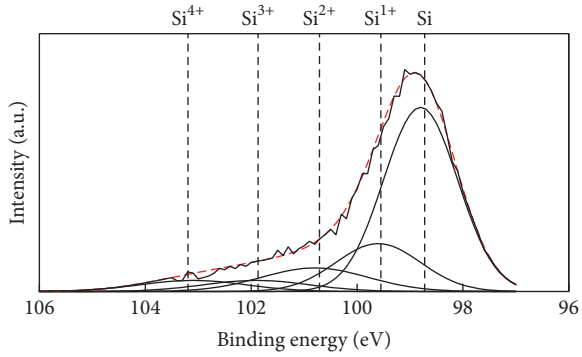

FIGURE 8: Si2*p* XPS spectrum of the composite.

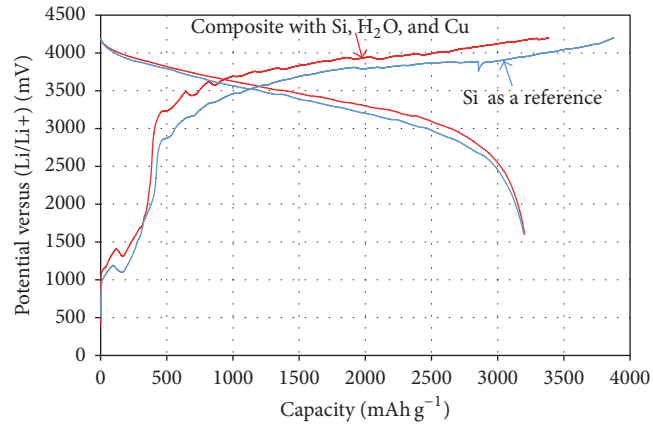

FIGURE 9: Charge-discharge capacity profiles of the composite anode (red) and a Si particle reference (blue).

of the particles. Approximately 75% of the XPS spectrum corresponds to Si and Si^{1+}, suggesting that the composite has a strong metallic character. Nearly 80% of all other oxidized species have oxidation numbers of Si^{2+} and Si^{3+}. The formation of Si monoxide or semimonoxide is expected owing to the controlled amount of H_2O added before the grinding process. These findings are evidence of the synthesis of Si monoxide or submonoxide, which are potentially useful as active materials in LIBs, based on oxidization reactions during grinding with H_2O.

2.2. Electrochemical Performance of the Composite. The electrochemical performance of the composite anode was evaluated in a 2032-type test coin cell using a constant current charge-discharge cycling test in the voltage range of 1.60–4.16 V with a current density of 0.1 mA cm^{-2} at room temperature. The state of charge was controlled at 100% in this study. As shown in Figure 9, the 1st charge-discharge capacity of the composite is more favourable than that using Si particles as a reference anode. The capacity was calculated using the weight of Si included in the anode of the coin cell. The 1st charge and discharge capacities for the composite were 3384 and 3160 mAh g^{-1}, respectively, whereas those for Si particles were 3871 and 3198 mAh g^{-1}, respectively.

The recharging capacity results indicate that the charge and reversible discharge capacities depend on the composition of the active material. The composite obtained by grinding Si, H_2O, and Cu demonstrated a 1st coulombic efficiency of 94.1% (Figure 10, red), whereas a 1st coulombic efficiency of 82.9% was observed when the anode only contained Si particles (Figure 10, blue). When the active material only contains Si, the 1st coulombic efficiency approaches 83% owing to formation of an irreversible solid electrolyte interphase (SEI), a chemical compound consisting of Li, Si, and solvent of electrolyte, on each Si particle, which does not work as an active material [1, 3]. Furthermore, Si crystals form amorphous or quasiamorphous Si phases after discharging Li ions, which have a lower capacity than the theoretical capacity of crystalline Si [5].

The composite produced by grinding Si, H_2O, and Cu was successfully employed as an anode to occlude Li ions. The composite is constructed of aggregates of Si, Si oxidation products, and Cu_3Si nanoscale particles, as indicated in Figure 5. We surmise that the Si nanoscale grains in the composite help to occlude Li ions with high coulombic efficiency during the first charge-discharge cycle; moreover,

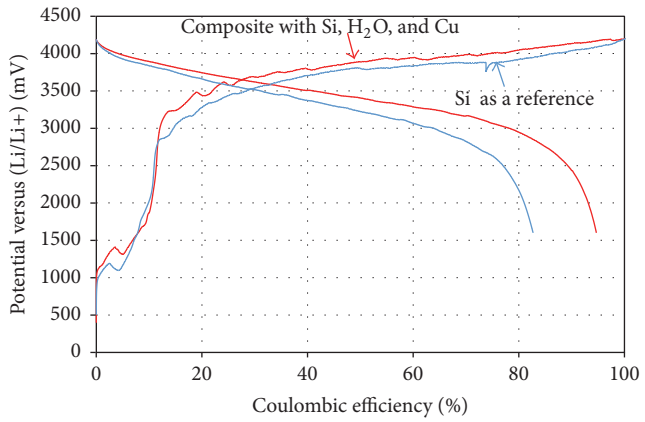

FIGURE 10: First coulombic efficiencies of the composite anode (red) and a Si particle reference (blue).

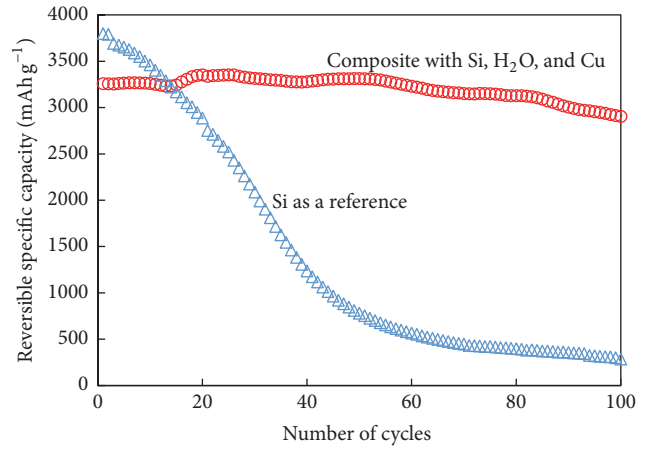

FIGURE 11: Cycling characteristics of the composite anode (red) and a Si particle reference (blue).

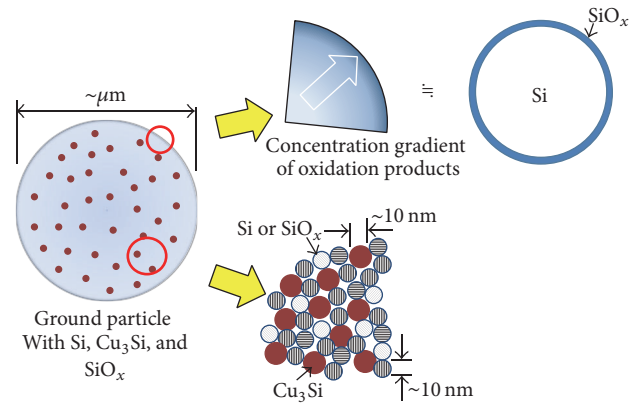

FIGURE 12: Schematic illustration of the composite formed by grinding Si, H_2O, and Cu. The composite can be modelled as an aggregate of Si, Cu_3Si nanoscale grains, and Si oxidation products near the surface, similar to a Si particle covered with a Si oxide film.

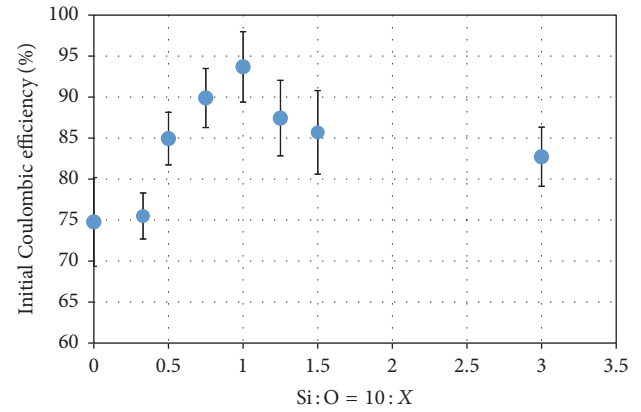

FIGURE 13: Change in initial coulombic efficiency with oxygen (as H_2O) addition ratio.

the Cu_3Si nanoscale grains act as an electrically conductive material. Further, to obtain good coulombic efficiency, the mixture of Si and Si monoxide prevents irreversible formation of an SEI [23–25]. In such mixtures, the optimized recharging efficiency and the conductivity of Si monoxide are lower than those of other Si oxides [26].

The cycling characteristics of the composite anode and a reference anode employing only Si particles are compared in Figure 11. The composite demonstrated a reversible capacity of over 3000 mAh g^{-1} after 100 cycles. Moreover, the capacity retention was over 99.9% for the 2nd cycle and 91.6% for the 100th cycle (Figure 11). In contrast, the bare Si particle anode had a low capacity retention of less than 50% over 40 cycles.

The monoxide or submonoxide Si species in the composite form near the surface, as shown in Figure 6. Thus, the structure of the composite was visualized as a Si active material covered by an oxide film. The optimization of the cycling characteristics by covering Si particles with an oxide film has been reported [26, 27]. The capacity retention was clearly found to be optimized by covering the active materials of the LIB anode with a thin film coating. It is believed that the film covering each Si particle plays a buffering role by preventing cracking following drastic changes in volume with numerous repetitions of the charge-discharge cycle. Based on our results, the composite has a structure consisting of aggregated Si, Cu nanoscale grains, and Si oxidation products, which accumulate as Si oxides at the surface of the composite and allow for optimization of the electrochemical characteristics of LIB cells, as shown in Figure 12.

The prepared composite sample exhibited nanostructures corresponding to both a Si matrix and Cu_3Si grains, which may be partly responsible for the improvement in battery performance, as reported in other studies on the preparation of nanostructured samples by various methods. However, we consider that there are other possible reasons for the improved performance of our composite sample. Notably, the extent of oxidization of the Si grains played an important role in increasing the coulombic efficiency, as revealed when we varied the ratio of H_2O to Si in the sample. Figure 13 shows the relationship between the initial coulombic efficiency and the molar ratio of Si to H_2O used during composite preparation. Without added H_2O, the coulombic efficiency was as low as

75%, but this value increased rapidly to 93.7% for a Si to H_2O ratio of 10 : 1. Further increasing the amount of H_2O led to a decrease in the coulombic efficiency. We postulated that higher amounts of H_2O during the mechanochemical reaction between Si, H_2O, and Cu would result in the production of a highly oxidized state of Si, with a higher ratio of SiO_2 in the obtained composite. Highly oxidized Si species such as SiO_2 tend to form stable Li silicates during the battery charging operation. When a Si to H_2O ratio of 10 : 1 was used for sample preparation, as shown in Figures 3–8, the obtained reaction product was SiO_x, where x is around 1 and much smaller than 2, as XPS analysis showed the formation of an amorphous layer around the crystalline Si grains. During lithiation, SiO_x with a low oxidation state will have a low tendency to react with Li to form silicates. On the other hand, the large increase in conductivity reported to be associated with low oxidation states of Si [26] will make the amorphous SiO_x layer more conductive than the Si matrix grains. Moreover, this layer acts as a physical buffer to reduce volume changes, thereby increasing efficiency.

3. Experimental

3.1. Synthesis of Composites of Si, H_2O, and Cu. As an excellent conductor, Cu_3Si has been widely studied for the improvement of Si anode performance through various modifications, such as coated layers on Si grains, and increased cycling efficiencies have been reported [28–31]. As shown in Figure 3, Cu_3Si nanoparticles with sizes of less than 10 nm are dispersed uniformly among the Si grains in our composite, which increases its conductivity. In addition to contributing to electronic conductivity, Cu_3Si may also serve as a good catalyst for increasing the cycling efficiency. There have been several reports on the catalytic effects of Cu_3Si in producing chlorosilanes from the reaction between CH_3Cl and Si [32]. Harper et al. have reported room-temperature oxidation of Si catalysed by Cu_3Si [33]. These studies indicate the high ability of Cu_3Si to catalyse the oxidation of Si to form chlorides or oxides. Although there have been no direct studies reporting the oxidation of Li silicides in anode materials, we believe that, in our prepared sample, the Cu_3Si nanoparticles dispersed uniformly around the Si grains, which exist as Li silicides after charging, will catalyse the oxidation of Li silicides and facilitate Li release, so that the rate of capacity fading is reduced. In addition to catalysis by Cu_3Si, the synergistic effects of the nanostructure of Si grains and the amorphous oxidized layers formed around the Si grains are considered to contribute to the observed high performance, with a capacity of over 3000 $mAh\,g^{-1}$ maintained after 100 cycles. The synergistic effects result from the mechanochemical approach, which is generally studied for stoichiometric reactions. However, in this case, nonstoichiometric ratios of H_2O and Cu were used to successfully prepare Si anode materials, expanding our understanding of mechanochemical phenomena.

4. Conclusion

Though it is necessary to employ Si as an active material to achieve both high charge and good cycling characteristics for charge-discharge performance, it is difficult to control Si active materials. We created a composite of active materials as an anode electrode for LIBs by compounding Si particles with H_2O and Cu particles using a grinding process. Oxidation-reduction reactions between Si and H_2O were activated by this process, resulting in Si oxidation. Thus, a composite containing aggregates of Si, Si oxidation products, and Cu_3Si nanoscale grains was achieved.

The Si oxidation number of the Si oxidation products could be controlled by the amount of H_2O added during grinding. Si monoxide was located near the surface of the composite, as revealed by EELS and XPS measurements. Therefore, the composite acts as an active material with high capacity and excellent charge-discharge properties over many cycles. Thus, we consider that further drastic improvement may be obtained from synergy effects when two or more actions are simultaneously introduced with only one operation. And this synthesis method for new anode materials and the battery, which has this anode, a commercial cathode, and an electrolyte, will be available for practical use in the commercial battery market.

While optimizing our treatment conditions for preparation of the Si composite, we are considering different applications of nonstoichiometric reactions to other similarly intricate issues. For example, we expect to be able to synthesis a cathode composite having more than three Li atoms in a molecule via the grinding process.

Conflicts of Interest

The authors declare that they have no competing interests.

Acknowledgments

The authors kindly thank DOWA Holdings Corporation for their help in the construction and electrochemical measurements of the composite employed in this study. The authors would like to thank Editage (https://www.editage.jp) for English language editing.

References

[1] A. Netz, R. A. Huggins, and W. Weppner, "The formation and properties of amorphous silicon as negative electrode reactant in lithium systems," *Journal of Power Sources*, vol. 119–121, pp. 95–100, 2003.

[2] K. Peng, J. Jie, W. Zhang, and S.-T. Lee, "Silicon nanowires for rechargeable lithium-ion battery anodes," *Applied Physics Letters*, vol. 93, no. 3, Article ID 033105, 2008.

[3] Y. Zhang, Z. Fu, and Q. Qin, "Microstructure and Li alloy formation of nano-structured amorphous Si and Si/TiN composite thin film electrodes," *Electrochemistry Communications*, vol. 6, no. 5, pp. 484–491, 2004.

[4] D. Munaò, M. Valvo, J. Van Erven, E. M. Kelder, J. Hassoun, and S. Panero, "Silicon-based nanocomposite for advanced thin film anodes in lithium-ion batteries," *Journal of Materials Chemistry*, vol. 22, no. 4, pp. 1556–1561, 2012.

[5] H.-Y. Lee and S.-M. Lee, "Carbon-coated nano-Si dispersed oxides/graphite composites as anode material for lithium ion

batteries," *Electrochemistry Communications*, vol. 6, no. 5, pp. 465–469, 2004.

[6] M. Mamiya, H. Takei, M. Kikuchi, and C. Uyeda, "Preparation of fine silicon particles from amorphous silicon monoxide by the disproportionation reaction," *Journal of Crystal Growth*, vol. 229, no. 1, pp. 457–461, 2001.

[7] K. Tahara, F. Iwasaki, T. Tamachi, and T. Sakai, *The 38th Battery Symposium in Osaka*, 1997.

[8] J. R. Dahn, S. Trussler, T. D. Hatchard et al., "Economical sputtering system to produce large-size composition-spread libraries having linear and orthogonal stoichiometry variations," *Chemistry of Materials*, vol. 14, no. 8, pp. 3519–3523, 2002.

[9] M. D. Fleischauer, T. D. Hatchard, G. P. Rockwell et al., "Design and testing of a 64-channel combinatorial electrochemical cell," *Journal of the Electrochemical Society*, vol. 150, no. 11, pp. A1465–A1469, 2003.

[10] V. K. Cumyn, M. D. Fleischauer, T. D. Hatchard, and J. R. Dahn, "Design and testing of a low-cost multichannel pseudopotentiostat for quantitative combinatorial electrochemical measurements on large electrode arrays," *Electrochemical and Solid-State Letters*, vol. 6, no. 6, pp. E15–E18, 2003.

[11] H. Yamamoto, M. Miyachi, and H. Kawai, "Abstracts of the Electrochemical Society of Japan 2004 Spring Meeting," Yokohama, pp. 204, 2004.

[12] T. Morita and N. Takami, "Nano Si cluster-SiO_x–C composite material as high-capacity anode material for rechargeable lithium batteries," *Journal of The Electrochemical Society*, vol. 153, no. 2, pp. A425–A430, 2006.

[13] M. Yamada, A. Ueda, K. Matsumoto, and T. Ohzuku, "Silicon-based negative electrode for high-capacity lithium-ion batteries: 'SiO'-carbon composite," *Journal of The Electrochemical Society*, vol. 158, no. 4, pp. A417–A421, 2011.

[14] Y. Ren, J. Ding, N. Yuan, S. Jia, M. Qu, and Z. Yu, "Preparation and characterization of silicon monoxide/graphite/carbon nanotubes composite as anode for lithium-ion batteries," *Journal of Solid State Electrochemistry*, vol. 16, no. 4, pp. 1453–1460, 2012.

[15] N. Dimov, S. Kugino, and M. Yoshio, "Mixed silicon-graphite composites as anode material for lithium ion batteries: influence of preparation conditions on the properties of the material," *Journal of Power Sources*, vol. 136, no. 2, pp. 108–114, 2004.

[16] M. Yoshio, T. Tsumura, and N. Dimov, "Silicon/graphite composites as an anode material for lithium ion batteries," *Journal of Power Sources*, vol. 163, no. 1, pp. 215–218, 2006.

[17] J.-H. Kim, H.-J. Sohn, H. Kim, G. Jeong, and W. Choi, "Enhanced cycle performance of SiO-C composite anode for lithium-ion batteries," *Journal of Power Sources*, vol. 170, no. 2, pp. 456–459, 2007.

[18] N. Shimoi, Z. Qiwu, S. Bahena-Garrido, and Y. Tanaka, "Mechanochemical approaches to employ silicon as a lithium-ion battery anode," *AIP Advances*, vol. 5, no. 5, Article ID 057142, 2015.

[19] Y. Tanaka, Q. Zhang, and F. Saito, "Mechanochemical dechlorination of trichlorobenzene on oxide surfaces," *Journal of Physical Chemistry B*, vol. 107, no. 40, pp. 11091–11097, 2003.

[20] Y. Hatanaka, S. Wickramanayaka, A. Matsumoto, Y. Nakanishi, and A. M. Wrobel, "Preparation of silicon based widegap semiconductor film from organo-silicon by using remote plasma CVD method," *Bulletin of the Research Institute of Electronics, Shizuoka University*, vol. 29, pp. 87–94, 1994.

[21] F. J. Himpsel, F. R. McFeely, A. Taleb-Ibrahimi, J. A. Yarmoff, and G. Hollinger, "Microscopic structure of the SiO_2/Si interface," *Physical Review B*, vol. 38, no. 9, pp. 6084–6096, 1988.

[22] F. Jolly, F. Rochet, G. Dufour, C. Grupp, and A. Taleb-Ibrahimi, "Oxidized silicon surfaces studied by high resolution Si 2p core-level photoelectron spectroscopy using synchrotron radiation," *Journal of Non-Crystalline Solids*, vol. 280, no. 1–3, pp. 150–155, 2001.

[23] M. Miyachi, H. Yamamoto, and H. Kawai, "Electrochemical properties and chemical structures of metal-doped SiO anodes for Li-ion rechargeable batteries," *Journal of the Electrochemical Society*, vol. 154, no. 4, pp. A376–A380, 2007.

[24] M. Miyachi, H. Yamamoto, H. Kawai, T. Ohta, and M. Shirakata, "Analysis of SiO anodes for lithium-ion batteries," *Journal of the Electrochemical Society*, vol. 152, no. 10, pp. A2089–A2091, 2005.

[25] Y. Nagao, H. Sakaguchi, H. Honda, T. Fukunaga, and T. Esaka, "Structural analysis of pure and electrochemically lithiated SiO using neutron elastic scattering," *Journal of the Electrochemical Society*, vol. 151, no. 10, pp. A1572–A1575, 2004.

[26] I. T. Johansen, "Electrical conductivity in evaporated silicon oxide films," *Journal of Applied Physics*, vol. 37, no. 2, pp. 499–507, 1966.

[27] N. Shimoi and Y. Tanaka, "Improvement in Si active material particle performance for lithium-ion batteries by surface modification of an inductivity coupled plasma-chemical vapor deposition," *Electrochimica Acta*, vol. 80, pp. 227–232, 2012.

[28] V. A. Sethuraman, K. Kowolik, and V. Srinivasan, "Increased cycling efficiency and rate capability of copper-coated silicon anodes in lithium-ion batteries," *Journal of Power Sources*, vol. 196, no. 1, pp. 393–398, 2011.

[29] S. Sim, P. Oh, S. Park, and J. Cho, "Critical thickness of SiO_2 coating layer on core@Shell bulk@nanowire Si anode materials for Li-ion batteries," *Advanced Materials*, vol. 25, no. 32, pp. 4498–4503, 2013.

[30] K.-F. Chiu, K. M. Lin, H. C. Lin, C. H. Hsu, C. C. Chen, and D. T. Shieh, "Electrochemical performances of Cu nanodots modified amorphous Si thin films for lithium-ion batteries," *Journal of the Electrochemical Society*, vol. 155, no. 9, pp. A623–A627, 2008.

[31] S. J. Jung, T. Lutz, A. P. Bell, E. K. McCarthy, and J. J. Boland, "Free-standing, single-crystal Cu_3Si nanowires," *Crystal Growth and Design*, vol. 12, no. 6, pp. 3076–3081, 2012.

[32] D.-H. Sun, B. E. Bent, A. P. Wright, and B. M. Naasz, "Chemistry of the direct synthesis of methylchlorosilanes from methyl + chlorine monolayers on a Cu_3Si surface," *Catalysis Letters*, vol. 46, no. 1-2, pp. 127–132, 1997.

[33] J. M. E. Harper, A. Charai, L. Stolt, F. M. d'Heurle, and P. M. Fryer, "Room-temperature oxidation of silicon catalyzed by Cu_3Si," *Applied Physics Letters*, vol. 56, no. 25, pp. 2519–2521, 1990.

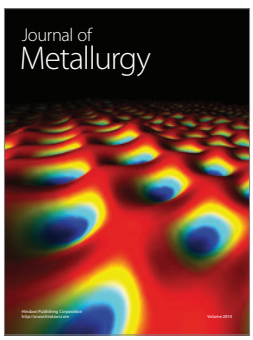

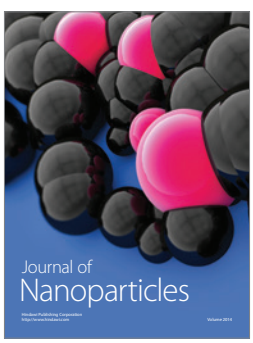

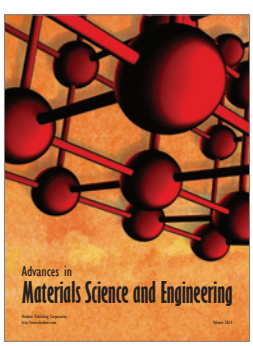

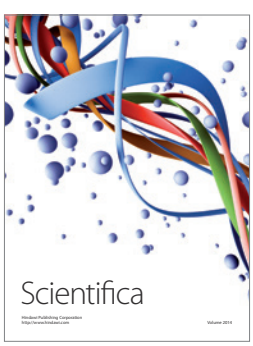

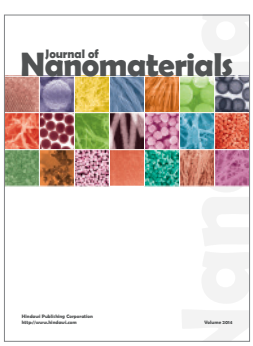

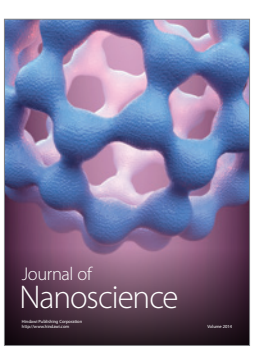

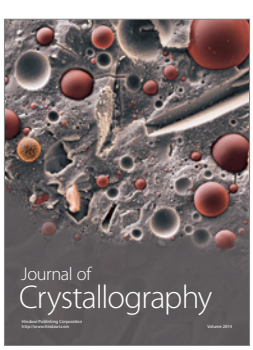

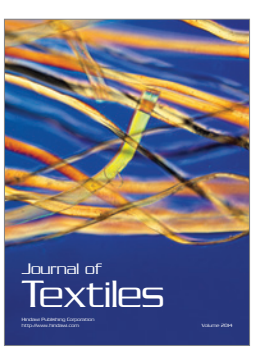

Hindawi

Submit your manuscripts at
https://www.hindawi.com